Chapter 7

Turbulent Combustion Modeling

7.1 Regimes of turbulent combustion

Numerous physical phenomena are involved in turbulent (premixed and non-premixed) combustion and different have been developed to capture them in the modeling depending on the combustion regimes. The premixed combustion regimes are identified according to key parameter diagram proposed in [32]. In the case of high intensity turbulence, the dispersion of

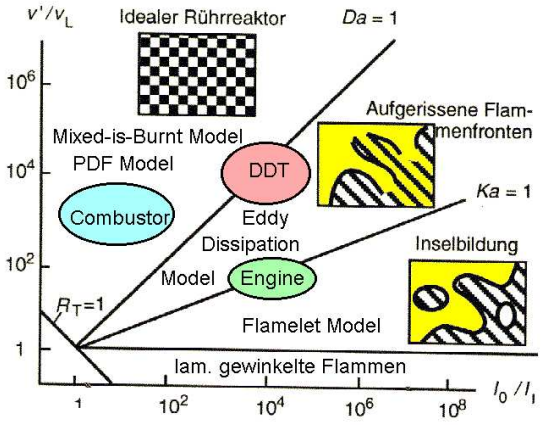

Figure 7.1: Diagram of turbulent combustion regimes.

fluid elements becomes sufficiently large to cause different portions of wrinkled flame sheets to approach each other. Laminar flame propagation may cause the reaction fronts to intersect and cut off pockets of unburnt gas. The flame front reconnection can be interpreted as a turbulent flame propagation, and formation of an archipelago of unburned gas pockets surrounded by combustion products could be a main consequences of chemistry-turbulence interaction. The transition from one regime of turbulent combustion to another is responsible to flame acceleration phenomenon because of the increase in flame surface area of the flamelets inside the turbulent structure. For sufficiently high level of turbulence, the flamelet structure maybe destroyed and replaced by a "distributed" reaction zone. Thus, under these conditions, turbulence exerts the main influence on the motion of the reaction zone, but chemical kinetics and molecular transport effects are never negligible.

7.2 Multi-component gas phase chemistry

The averaged gas phase equations for a chemically reacting mixture of ideal gases with embedded condensed liquid droplets can be written as

$$\frac{\partial \rho Y_k}{\partial t} + \nabla[\rho Y_k \vec{u} - \frac{\mu_t}{Sc_k}\nabla Y_k] = \dot{\rho}_k^c + \dot{\rho}_k^s, \quad k = 1, ..., N_s \tag{7.1}$$

where $\dot{\rho}_k^c$ is the chemical source term defined by combustion mechanism.

The N_r elementary chemical reactions involving N_s species X_s are represented in the form

$$\sum_{s=1}^{N_s} \nu'_{sr} X_s \underset{k_b^r}{\overset{k_f^r}{\rightleftharpoons}} \sum_{s=1}^{N_s} \nu''_{sr} X_s \quad , r = 1, N_r. \tag{7.2}$$

Here X_s stands for one mole of s-species, and ν'_{sr} and ν''_{sr} are stoichiometric coefficients for the r-th reaction.

Formal kinetics requires $\nu'_{sr} \cdot \nu''_{sr} = 0$, i.e. species "s" is formed only from the other species. The chemical mass production terms in the mass balance eqs (4) are

$$\dot{\rho}_s = M_s \sum_{r=1}^{N_r} (\nu''_{sr} - \nu'_{sr}) \dot{\omega}_r, \tag{7.3}$$

and the chemical heat release term in the internal energy equation is given by

$$\dot{Q}_c = \sum_{r=1}^{N_r} q_r \dot{\omega}_r, \tag{7.4}$$

where q_r is the heat of r-reaction at $T = T_{ref}$,

$$q_r = \sum_s (\nu'_{sr} - \nu''_{sr})(h_s)_f^o. \tag{7.5}$$

The variable $\dot{\omega}_r$ is the rate of progress of the r-th reaction:

$$\dot{\omega}_r = k_f^r(T) \prod_{k=1}^{N_s} (\frac{\rho_k}{M_k})^{\nu'_{kr}} - k_b^r(T) \prod_{k=1}^{N_s} (\frac{\rho_k}{M_k})^{\nu''_{kr}}, \tag{7.6}$$

where T is the temperature, k_f^r and k_b^r are the rate coefficients for forward and backward stages of the r-reaction. The rate multipliers k_f^r and k_b^r are used, as a rule, in a generalized Arrhenius form

$$\begin{aligned} k_f^r &= a_f^r T^{\zeta_f^r} exp(-T_{af}^r/T) M_r, \\ k_b^r &= a_b^r T^{\zeta_b^r} exp(-T_{ab}^r/T) M_r, \end{aligned} \tag{7.7}$$

with the equilibrium constraint

$$k_f^r = k_b^r K_e^r(T), \tag{7.8}$$

where K_e^r is the equilibrium constant in concentration units, and the third body factor, M_r, defined as

$$M_r = \begin{cases} \sum_m^{N_s} \rho_m / W_m \beta_{r,m} & \text{for third body reactions} \\ 1.0 & \text{otherwise} \end{cases} \tag{7.9}$$

where $\beta_{r,m}$ are the third body efficiencies for m-species in r-reaction.

7.2.1 Mechanism of hydrogen combustion in oxygen (air)

Hydrogen/oxygen combustion, which powers e.g, the space shuttle, is nearly the most powerful chemical reaction known and the combustion mechanism has been studied for decades. The finite-rate H_2/O_2 combustion mechanism, (8 species, 26 reactions), and reaction rate parameters in the Arrhenius form are listed in Table 1 and based mainly on the data in [**?**]. The chaperon efficiencies for the third body concentrations M_r are defined by following expressions: β_{1,H_2}= β_{2,H_2}=2.5, β_{1,H_2O}=12.0, β_{2,H_2O}=15.0. Rate coefficients for the backward reactions are computed with the help of linear regression by satisfying of the constraint (7.8). Stages 27-31 included in the Table 1 represent chemically equilibrium mechanism used in the rocket propulsion modeling.

The mechanism was tested by comparing computed results with the experimental data [**?**] for ignition delay times of stoichiometric H_2/Air mixtures at 2 atm, (see Fig. 7.2a). Although experimental data for rocket chamber conditions are not available in literature, relevant data for highly diluted (by Ar) stoichiometric mixtures obtained using a new high-pressure shock

Table 1
Reaction Mechanism for H_2/O_2 Combustion

Reaction	a_f^r	ζ_f^r	E_{af}^r
$1. H_2 + O_2 \rightleftharpoons OH + OH$	$1.7 \cdot 10^{13}$	0.0	47780.
$2. H_2 + OH \rightleftharpoons H_2O + H$	$1.2 \cdot 10^{09}$	1.30	3626.
$3. O + OH \rightleftharpoons O_2 + H$	$4.0 \cdot 10^{14}$	-0.50	0.
$4. O + H_2 \rightleftharpoons OH + H$	$5.0 \cdot 10^{04}$	2.67	6290
$5. H + HO_2 \rightleftharpoons O + H_2O$	$3.1 \cdot 10^{10}$	0.0	3590.
$6. O + OH + M \rightleftharpoons HO_2 + M$	$1.0 \cdot 10^{16}$	0.0	0.
$7. H + O_2 + M_2 \rightleftharpoons HO_2 + M_2$	$3.6 \cdot 10^{17}$	-0.72	0.
$8. OH + HO_2 \rightleftharpoons H_2O + O_2$	$7.5 \cdot 10^{12}$	0.0	0.
$9. H + HO_2 \rightleftharpoons OH + OH$	$1.4 \cdot 10^{14}$	0.0	1073.
$10. O + HO_2 \rightleftharpoons O_2 + OH$	$1.4 \cdot 10^{13}$	0.0	1073.
$11. OH + OH \rightleftharpoons O + H_2O$	$6.0 \cdot 10^{08}$	1.3	0.
$12. H + H + M_1 \rightleftharpoons H_2 + M_1$	$1.0 \cdot 10^{18}$	-1.0	0.
$13. H + H + H_2 \rightleftharpoons H_2 + H_2$	$9.2 \cdot 10^{16}$	-0.6	0.
$14. H + H + H_2O \rightleftharpoons H_2 + H_2O$	$6.0 \cdot 10^{19}$	-1.25	0.
$15. H + OH + M \rightleftharpoons H_2O + M$	$1.6 \cdot 10^{22}$	-2.0	0.
$16. H + O + M \rightleftharpoons OH + M$	$6.2 \cdot 10^{16}$	-0.6	0.
$17. O + O + M \rightleftharpoons O_2 + M$	$1.9 \cdot 10^{13}$	0.0	$-1788.$
$18. H + HO_2 \rightleftharpoons H_2 + O_2$	$1.2 \cdot 10^{13}$	0.0	0.
$19. HO_2 + HO_2 \rightleftharpoons H_2O_2 + O_2$	$2.0 \cdot 10^{12}$	0.0	0.
$20. H_2O_2 + M \rightleftharpoons OH + OH + M$	$1.3 \cdot 10^{17}$	0.0	45500.
$21. H_2O_2 + H \rightleftharpoons HO_2 + H_2$	$1.6 \cdot 10^{12}$	0.0	3800.
$22. H_2O_2 + H \rightleftharpoons H_2O + OH$	$1.0 \cdot 10^{13}$	0.0	3590.
$23. H_2O_2 + OH \rightleftharpoons H_2O + HO_2$	$1.0 \cdot 10^{13}$	0.0	1800.
$23. H_2O_2 + H \rightleftharpoons H_2O + OH$	$1.0 \cdot 10^{13}$	0.0	3590.
$24. H_2O_2 + O \rightleftharpoons H_2O + O_2$	$8.4 \cdot 10^{11}$	0.0	4260.
$25. H_2O_2 + O \rightleftharpoons OH + HO_2$	$2.0 \cdot 10^{13}$	0.0	5900.
$26. HO_2 + H_2 \rightleftharpoons H_2O + OH$	$6.5 \cdot 10^{11}$	0.0	18800.
$27. O_2 \rightleftharpoons O + O$	1.0		
$28. H_2 \rightleftharpoons H + H$	1.0		
$29. H_2 + O_2 \rightleftharpoons OH + OH$	1.0		
$30. H_2O + OH \rightleftharpoons HO_2 + H_2$	1.0		
$31. H_2O + H_2O \rightleftharpoons H_2O_2 + H_2$	1.0		

The table consists of two blocks for elementary and equilibrium reactions, respectively. Rate coefficients, third body concentrations M_i and chaperon efficiencies are taken in the form of [**?**].

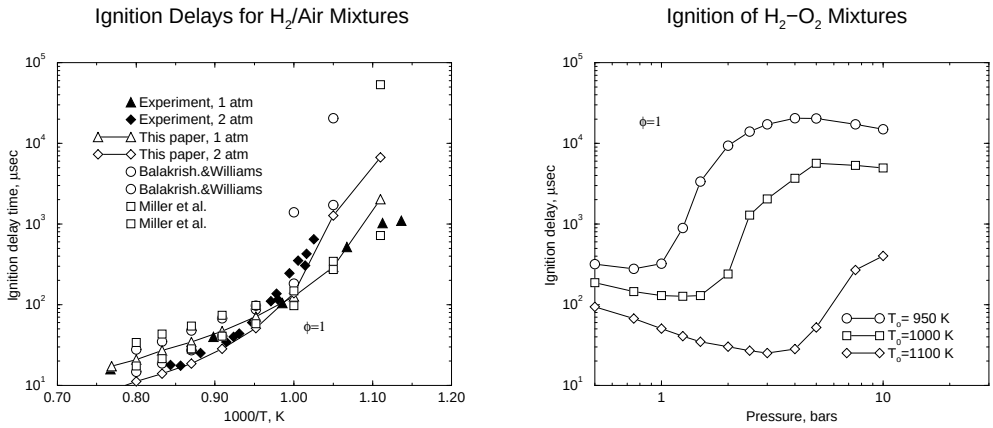

(a) (b)

Figure 7.2: a) Calculated ignition delays for the stoichiometric H_2/O_2 mixture vs shock-tube experimental data; b) non-monotonous dependence of ignition delays on pressure for different initial temperatures.

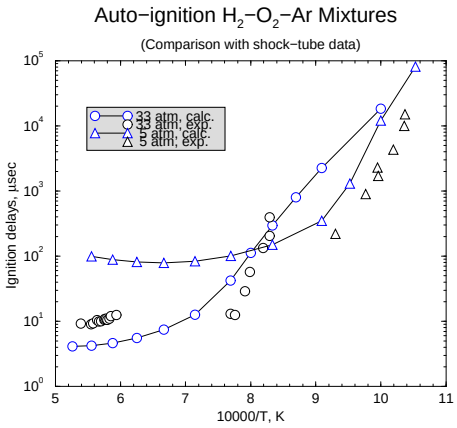

Figure 7.3: Predicted and measured (in shock tube experiments) ignition delay times for stoichiometric H_2/O_2/Ar mixtures at elevated pressures.

tube [49] (stoichiometric mixtures for pressures between 33 and 87 atm [1] and temperatures from 1175 to 1880 K) were compared with predictions, and the results of such a comparison are presented in Fig. 7.3. The measured ignition delays are insensitive to inert-gas dilution for Ar levels (95.0-99.85 %) used in the experiments. At high temperatures, the ignition delays are practically independent on pressure, but they turn out to be very sensitive to pressure levels at high temperatures. Ignition delays are less sensitive to pressure level at low temperatures.

A sensitivity analysis (based on the SENKIN code of the Chemkin-2 library) applied to this reaction mechanism study shows that at low pressures the ignition process is well controlled by the classic H_2/O_2 combustion mechanism, (reaction 3 in Table 1 dominates), while at high pressures, the role of the trimolecular reaction 7 becomes more pronounced during the induction period. The competition between reactions 3 and 7 explains the non-monotonous dependence

[1]The 5 atm data of Skinner and Ringrose are added for completeness

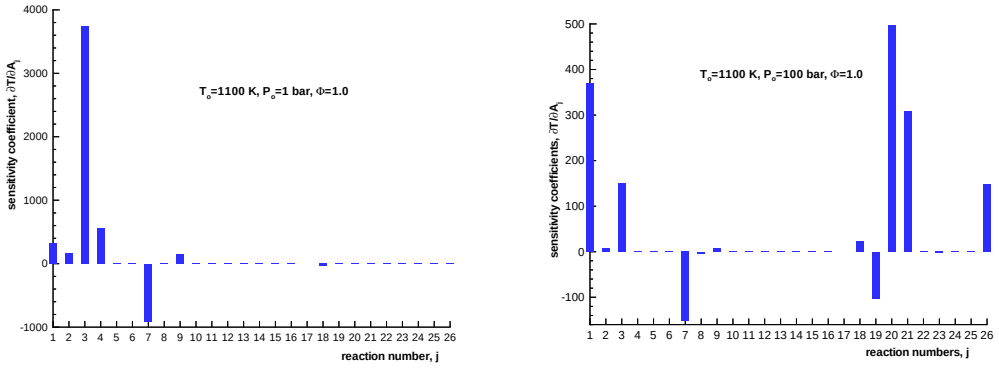

(a) (b)

Figure 7.4: Absolute sensitivity coefficients for the H_2/O_2 reaction mechanism of Table 1 at the end of ignition period (t_{id}=3.0·10^{-5} sec): a) atmospheric pressure case, b) high pressure case.

of ignition delays on the pressure presented in Fig. 7.2b and the other peculiarities of ignition at high pressures.

7.2.2 Motor fuel surrogates models

The word **"fuels"**, see [17], refers to a range of products refined from crude oil,which are usually liquids (occasionally gasses), that burn in the presence of air and enable the operation of heat engines, either rocket, piston (mainly gasoline and diesel) or turbine (aircraft engines). Practical diesel fuels consist of a great number of aliphatic and aromatic compounds, and their combustion is too complex to be modeled using a comprehensive chemical mechanism. Instead of this, the model or surrogate fuels are used in numerical simulations. Aliphatic components can be represented by long chain hydrocarbons such as n-heptane or n-dodecane to their cetane number of approximately $\sim$ 56, which is similar to the cetane number of conventional diesel fuel. Aromatic components significantly contribute to soot formation. The diesel fuel surrogate,

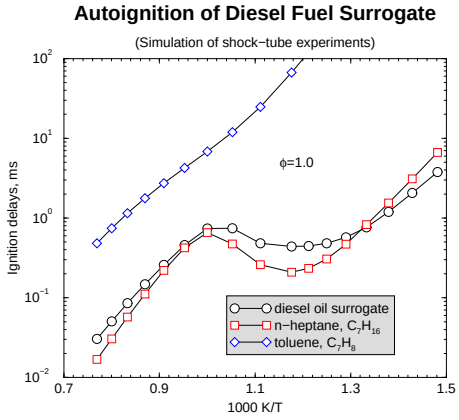

Figure 7.5: Ignition delays for fuel surrogate and its components simulating shock tube experiments; p$_o$=41.0 bar, ϕ = 1 for all compounds.

which can sufficiently represent the cetane number as well as the other properties of real fuel is assumed to be a 70/30 % mixture of n-heptane, C_7H_{15}, and toluene, C_7H_8. The alternative model consisting of the mixture of n-dodecane and α-methylnaphthalene was also proposed. If the physical properties of the model fuel are represented by properties of real diesel oil, the difference in combustion models seems not critical.

At first, detailed reaction mechanisms for n-heptane and toluene oxidation have been developed and validated using shock-tube auto-ignition experimental data. Such a detailed mechanism integrating the n-heptane and toluene oxidation chemistry with the kinetics of aromatics (up to four aromatic rings) formation for rich acetylene flames by [15] was, then, reduced on the bases of sensitivity analysis (using the software of the Chemkin-2 [4] package) to the mechanism consisting of 68 species participating in 280 reactions which implemented into the KIVA-3V code [42]-[43] to simulate diesel spray combustion. This mechanism was assumed to predict the fuel auto-ignition, combustion development and formation of polycyclic aromatic hydrocarbons (PAHs) till gaseous soot precursors based on acenaphthylene, A2R5, which are non-planar aromatic rings. The mechanism for both aliphatic and aromatic components includes principal fragments of C_1-C_7 and O/H chemistry taken from different sources, but mainly from LLL [44] and MIT [45] databases. More detailed discussion of the fuel surrogate models can be found in the Appendix III.

7.2.3 Soot formation model based on PAH concept

Soot formation mechanism consists of series of elementary reaction steps leading from acetylene and hydrogen to the formation of the first aromatic ring, A_1. Reaction steps leading to the formation of the phenyl, $A_1^{\bullet}$, radical and the first aromatic ring are followed by the successive stages of H- abstraction, C_2H_2- addition (HACA- mechanism), thus, yielding a chain of aromatic rings. Toluene can form A_1 without the presence of acetylene. A special reaction sequence was included leading via benzene dimerization to acenaphthylene. The incipient soot was formed from long-chain acetylene, C_6H_2, and acenaphthylene via "graphitization" processes

$$\begin{aligned} C_6H_2 &\rightharpoonup H_2 + 6C(s) \\ A_2R5 &\rightharpoonup 4H_2 + 12C(s) \end{aligned} \tag{7.10}$$

The notation C(s) + H_2 can be formally attributed to incipient soot as the latter contains a significant amount of hydrogen. Thermal properties of C(s) have been taken as properties of graphite. The complete reaction mechanism and species thermodynamic property are provided by [46]. The physical properties of the fuel surrogate were taken as properties of real fuel compiled in the DI model of the KIVA-3V fuel library with the original fuel chemical formula replaced by $C_{14}H_{28}$.

Soot formation mechanism consists of series of elementary reaction steps leading from acetylene and hydrogen to the formation of the first aromatic ring, A_1. Reaction steps leading to the formation of the phenyl, $A_1^{\bullet}$, radical and the first aromatic ring are followed by the successive stages of H- abstraction, C_2H_2- addition (HACA- mechanism), thus, yielding a chain of aromatic rings. Toluene can form A_1 without the presence of acetylene. A special reaction sequence was included leading via benzene dimerization to acenaphthylene. The incipient soot was formed from long-chain acetylene, C_6H_2, and acenaphthylene via "graphitization" processes

$$\begin{aligned} C_6H_2 &\rightharpoonup H_2 + 6C(s) \\ A_2R5 &\rightharpoonup 4H_2 + 12C(s) \end{aligned} \tag{7.11}$$

The notation C(s) + H_2 can be formally attributed to incipient soot as the latter contains a significant amount of hydrogen. Thermal properties of C(s) have been taken as properties of graphite. The complete reaction mechanism and species thermodynamic property are provided by [46]. The physical properties of the fuel surrogate were taken as properties of real fuel compiled in the DI model of the KIVA-3V fuel library with the original fuel chemical formula replaced by $C_{14}H_{28}$.

7.3 Multi-component molecular diffusion

Diffusion transport in the N-component gas mixture is governed by the system of equations:

$$\sum_{j\neq i}^{N}(x_i x_j)/D_{ij}(\mathbf{u_j}-\mathbf{u_i}) = \nabla x_i, \quad i=1,...,N \tag{7.12}$$

where $\mathbf{u}_i$ is the i-th species specific velocity, x_i is the mole fraction of i-th species, D_{ij} is the binary diffusivity of the pair (i,j).

If specific velocities are defined from the system (7.12), the diffusion fluxes $\mathbf{J}_i$ relative to the mass averaged velocity $\mathbf{u}$ needed for closure of the mass and energy conservation laws of fluid mechanics can be calculated as

$$\mathbf{J_i} = \rho_i(\mathbf{u_i}-\mathbf{u}), \quad i=1,...,N \tag{7.13}$$

where ρ_i is the partial mass density of i-th species.

In the system (7.12), only N-1 equations are linearly independent, as their sum over i yields **0=0**. Thus, the determinant of the system (7.12) is equal to 0, and a unique solution for this system does not exist. The lack of the solution uniqueness is due to the fact that Eqs (7.12) involve only velocity differences, and there is no information about absolute velocities. The latter information is contained in the equation defining the mass-averaged velocity. If this velocity is defined as

$$\mathbf{u} = \sum_{i}^{N}(\rho_i/\rho)\mathbf{u_i}, \tag{7.14}$$

the diffusion fluxes identically sum to zero., i.e

$$\sum_{i}^{N}\mathbf{J_i} = 0 \tag{7.15}$$

7.4 Chemistry/turbulence interaction

The direct implementation of the approach described above for the particular chemical mechanism in the CFD codes sometimes is restrictive due to the computer time and memory constraints. Moreover, this approach known as the quasi-laminar model does not included the effect of turbulence on chemical reactions. Till recently, there was no explicit coupling of chemical kinetics and the rate of combustion in entirely turbulent mixing-controlled regime. In particular, in [33] was proposed a method which requires only the evaluation of averaged species mass fractions to describe chemical kinetics, albeit in a very simple form, in the course of the pre-combustion period. Let us analyze this model (known as the Eddy Dissipation Concept, EDC, in more details.

The original EDC model of [33] assumes a one-step global reaction such as

$$(1kg)fuel + (\sigma kg)oxidizer \rightarrow (1 + \sigma kg)products,$$

where σ is the stoichiometric ratio of mass of oxidizer to that of fuel.

Although an application of the original EDC model to multi-reaction mechanism is, in principle, possible, it meets some difficulties. They are not only because of the fact that in the past, this has been dictated only by the fact that till recently, the integrations of large-scale chemical mechanisms with 3D CFD models were far beyond the capabilities of practical simulations. The Eddy Dissipation Concept (EDC) is the model which can facilitate the efforts making this integration a reality. However, the EDC combustion model was not yet analyzed in detail, albeit the model is said to be implemented in practically all commercial codes available. For example, in the latest review by Veynante and Vervisch published recently in [31], the model has been referred as belonging to the family of "infinitely fast chemistry" models and summarized in only 15 half-lines of the following text: "The eddy dissipation model (EDC) is a direct extension to non-premixed flame of the eddy break up (EBU) closure initially devoted to turbulent premixed combustion... The fuel burning rate is calculated according to:

$$\overline{\rho\dot{w}_{f,edc}} = -\alpha\bar{\rho}\frac{\epsilon}{k}min(\tilde{Y_f}, \frac{\tilde{Y_o}}{s}, \beta\frac{\tilde{Y_p}}{1+s}), \tag{7.16}$$

where α and β are adjustable parameters of the closure". In the above equation, "... the reaction rate is limited by a deficient species. To account for the existence of burnt gases bringing the energy to ignite the fresh reactants, this species may be the reaction product (when β is non-zero)... Actually, for large α, the model is difficult to justify."

It is clear that the above review attributes the EDC model only to its first, Magnussen and Hjertager, M-H, formulation [33], but even this version of the model was not amply covered in the literature. The reaction product term (when β is non-zero) is introduced into the rate expression to account for finite-rate chemistry effects (ignition/quenching) that makes it incorrect to place the EDC approach in the family of "infinitely fast chemistry" models. In fact, the actual reaction rate is taken to be in a very controversial form

$$\dot{\omega}_j = min(\dot{\omega}_c, \dot{\omega}_{edc}) \tag{7.17}$$

argued by "heuristic" considerations to extend the approach to multi-step reaction mechanisms.

When the reaction rates are determined, the source terms in the species conservation equations are defined as

$$\dot{\rho}_k^c = M_k \sum_{j=1}^{N_r} (\nu''_{k,j} - \nu'_{k,j})\dot{\omega}_{j,k}, \tag{7.18}$$

and the chemical heat release term in the energy equations becomes

$$\dot{Q}^c = \sum_{j=1}^{N_r} Q_j \dot{\omega}_j, \tag{7.19}$$

where Q_j is the negative of the j-reaction heat at the reference temperature defined as

$$Q_j = \sum_k (\nu''_{k,j} - \nu'_{k,j})(\Delta h_f^o)_k, \tag{7.20}$$

where $(\Delta h_f^o)_k$ is the heat of formation of k-species at the reference temperature.

Some other versions of so called EDC model, e.g., [35] were formulated without a proper connection with the original EDC approach. Also, Fluent [36] claimed the implementation of a new version of the EDC model "...for the modeling of turbulent finite-rate chemistry. It is completely different from the eddy dissipation model that has long been available."

The section below is aimed to fill a gap in the EDC based models analysis starting with an outline of the classic EDC model features. *The basic assumption of the EDC is that chemical reactions occur only in the turbulence fine structure, i.e., Kolmogorov size eddies and that the reactions are quenched, if the characteristic chemical times for limiting species are longer than the Kolmogorov time*. Thus, the classic EDC model does not allow the reaction zone broadening beyond the Kolmogorov limit.

7.4.1 Formulation of the new EDC Model

The new model formulation is based on the operator-splitting procedure (see Appendix II) applied to the mass conservation equations for species participating in any multi-step reaction mechanism. In terms of this approach, the time differencing was performed in three steps: the first step was assumed to be the convection contribution, the second one - diffusion effect without a contribution of micro-mixing, and the third step was the chemical kinetics effect coupled with micro-mixing. The last step of such a mass balance can be interpreted as representing combustion in a *constant volume* partially stirred reactor (PaSR) of a computational cell size, where reactions occur in a fraction of its volume. Since the reaction zone parameters, as a rule, can not be resolved on a computational grid, the sub-grid diffusion term due to micro-mixing was approximated with the help of introduction of a micro-mixing time as suggested in the "interaction with the mean" approach [37]. Then, assuming that chemical processes proceed in such a way that the shortest chemical time associated with particular (reference) species participating in the reaction was constrained by the micro-mixing time, a system of PaSR equations consisting of two sets (first - differential, second - algebraic) can obtained

$$\frac{dc^1}{dt} = \frac{c^1 - c^o}{\tau} = -\frac{c}{\tau_c}, \quad \frac{c - c^1}{\tau_{mix}} = -\frac{c}{\tau_c}, \tag{7.21}$$

where τ is the time step, τ_c is the chemical reaction time, and τ_{mix} is the micro-mixing time. The model distinguishes (see Fig. 2) between the concentration (in mean molar density) at the reactor exit, c^1, the concentrations in the reaction zone, c, and in the feed, c^0. When time proceeds, c^1 trades place for c^0.

After algebraic manipulations, one can yield the analytical solutions of the above problem

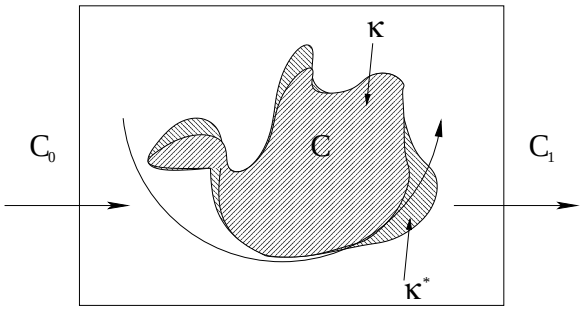

Figure 7.6: Partially stirred reactor, PaSR, consisting of non-premixed, premixed, and premixed and reactive regions.

which, finally, can be represented as

$$\frac{c^1 - c^o}{\tau} = -(\frac{c^1}{\tau_c}) \cdot \kappa = -\frac{1}{2} H(\frac{c^1}{\tau_c}, \frac{c^1}{\tau_{mix}}), \tag{7.22}$$

where $\kappa = \tau_c/(\tau_{mix} + \tau_c)$, and H is a harmonic mean.

The solution (7.22) shows that the turbulent combustion time is *a sum of the mixing and reaction times*, if the process is expressed in terms of the reactor output parameters. This is the main consequence of the PaSR model.

For the detailed chemical mechanism, the species production rate due to the particular r-chemical reaction (separated into creation and destruction rates) contrary to the first equation of the system (7.21) can be rewritten as

$$\frac{dc^1}{d\tau} = f_r(c) = \frac{c - c^1}{\tau_{mix}} \tag{7.23}$$

where

$$f_r(c) = (\nu_r'' - \nu_r')\dot{\omega}_r(c) = term_r^{\oplus} - term_r^{\ominus}$$

where ν_r'' and ν_r' are stoichiometric coefficients of the backward and forward stages, $\dot{\omega}_r$ is a progress variable rate of the r-reaction . Species indices are omitted for simplification.

The reaction progress variable rate $\dot{\omega}_r(c)$ is calculated from the mass-action law

$$\dot{\omega}_r(c) = k_f^r(T) \prod_{s=1}^{N_s} (c_s)^{\nu'_{sr}} - k_b^r(T) \prod_{s=1}^{N_s} (c_s)^{\nu''_{sr}},$$

where k_f^r and k_b^r are the rate coefficients for the forward and backward stages of the r-reaction, T is the temperature, and N_s is the total number of species in the mixture. here is a substantial difference between Eqs (7.21) and (7.23) - the original model has the analytical solution, while the application of the second one requires numerical integration. Combination of the terms in the model (7.23) leads to a definition of the reactive volume as introduced in [48]:

$$c^1 = c\kappa^* + c^o(1 - \kappa^*), \tag{7.24}$$

where the multiplier $\kappa^* = \tau/(\tau + \tau_{mix})$, while τ is the integration step.

Rewriting the first relation of (7.23) in terms of the reactor exit parameters, one can get

$$\begin{aligned} \frac{c^1 - c^o}{\tau} &= f_r(c) \simeq f_r(c^1) + (\partial f_r/\partial c)_{|c=c^1}(c - c^1) \\ &= f_r(c^1) - \frac{c - c^1}{\tau_c} \end{aligned}$$

The rhs of the above equation is constructed using Taylors expansion at the state c^1, assuming that the reaction times can be estimated as reciprocal values of elements of the Jacobian matrix evaluated at unknown values c=c^1, i.e., $\tau_c \sim [\partial f_r/\partial c]^{-1}$ and that $(\partial f_r/\partial c)_{|c=c^1} < 0$. Elimination of c-values using c^1-values taken from Eq. (7.24)

$$\frac{c^1 - c^o}{\tau} = f_r(c^1) - [\frac{c^1}{\kappa^*} - \frac{c^o(1 - \kappa^*)}{\kappa^*} - c^1]/\tau_c, \tag{7.25}$$

if the reaction time is defined as

$$\tau_c{}^{-1} = -f_r{}^o/(c_s{}^o + term_r^{\ominus}\tau),$$

immediately puts the reaction rate into the form

$$\begin{aligned}\frac{c^1 - c^o}{\tau} &= f_r(c^1) \cdot \frac{\tau_c}{\tau_c + \tau_{mix}} \\ &= \frac{{c_s}^o {f_r}^o}{{c_s}^o + term_r^{\ominus}\tau + term_r^{\ominus}\tau_{mix}},\end{aligned} \tag{7.26}$$

containing no reaction zone parameters c which cannot be resolved on a grid, but replacing their effect with the rate multiplier κ. The superscript ^{o} and the subscript $_s$ denotes the value at the start of the integration step and the "reference" species index defined below.

This expression looks different from the original finite-rate formulation of the EDC model known as

$$\overline{\rho \dot{w}_s} = \frac{\kappa_M}{1 - \kappa_M} \cdot \frac{c_s^* - c_s^1}{\tau_{mix}}, \tag{7.27}$$

where κ_M is the fine structure volume, and * denotes the fine-structure quantities, but a generic proximity of the approximations can be established using the PaSR formulation.

The chemical reaction times are formally defined as characteristic times of the destruction rates, if the species chemical production rates are presented as a sum of creation and destruction terms. In this way, for each reaction of the mechanism, chemical times can be attributed to each species participating in the depletion stages, e.g., -$k_r c_i c_k \approx -c_i/\tau_{c,i} \approx -c_k/\tau_{c,k}$, where i, k are species indices. In terms of the EDC model, the shortest of these times is restricted from below by the micro-mixing time that explains the usage of deficient (limiting) species in the rate expression (7.16).

Application of the rate expression (7.26) to a linear approximation of the Arrhenius reaction:

$$f_r^o = -c_s^o/\tau_c$$

leads to the formula

$$\begin{aligned}\frac{c_s^o f_r^o}{c_s^o + term_r^{\ominus}\tau + term_r^{\ominus}\tau_{mix}} &= -\frac{c_s^o}{\tau + \tau_c + \tau_{mix}} \\ = -\frac{c_s^1}{\tau_c + \tau_{mix}} &= -\frac{1}{2} H(\frac{c_s^1}{\tau_c}, \frac{c_s^1}{\tau_{mix}})\end{aligned}$$

which is perfectly consistent with the PaSR analytical solution (7.22). In a limiting case of chemical equilibrium, the model automatically approaches the M-H model.

7.4.2 Reference species definition

The reference species is similar to the limiting species used in the M-H model [33] by defining the reaction rates. Let us consider the balance equation of s-species participating in the r-reaction:

$$\begin{gathered}\frac{c_s^1 - c_s^o}{\tau} = (\nu''_{sr} - \nu'_{sr})[k_f^r(T)\Pi_1 - k_b^r(T)\Pi_2] = \\ \underbrace{[\nu'_{sr} k_b^r \cdot \Pi_2 + \nu''_{sr} k_f^r \cdot \Pi_1]}_{term_r^{\oplus}} - \underbrace{[\nu'_{sr} k_f^r \cdot \Pi_1 + \nu''_{sr} k_b^r \cdot \Pi_2]}_{term_r^{\ominus}},\end{gathered}$$

where

$$\Pi_1 = \prod_{n=1}^{N_s} (c_n^1)^{\nu'_{nr}},\ \Pi_2 = \prod_{n=1}^{N_s} (c_n^1)^{\nu''_{nr}},$$

The above equation written in a form separating the net chemical production rate into creation and destruction terms is assumed to be linearized as

$$\begin{aligned} \frac{c_s^1 - c_s^o}{\tau} &= f^r(t, c_s^1) = term_r^{\oplus} - term_r^{\ominus}\frac{c_s^1}{c_s^o} \\ c_{s|\tau=0}^1 &= c_s^o, \end{aligned} \tag{7.28}$$

This linearized expression is mostly accurate for the species which concentration is less than those of the other reaction partners. Thus, such a species (called reference species) is playing a special role in the analysis. The factor before this species has a dimensional representation of an inverse time. This time is the shortest time for the particular reaction. By algebraic manipulation with Eq. (7.28), one can get the expressions for unknown terms in Eq. (7.26), viz., $f_r(c^1)$ and τ_c:

$$\begin{aligned} f^r(c_s^1) &= \frac{c_s^o f_o^r}{c_s^o + term_r^{\ominus}\tau}, \\ {\tau_c}^{-1} &= -(\partial f^r/\partial c)_{|_{c=c_1}} \approx -{f_r}^o/({c_s}^o + term_r^{\ominus}\tau) \end{aligned}$$

As shown in [48], introduction of reference species assures the equilibrium conditions implementation at $\tau \to \infty$ for each reaction in the mechanism.

7.4.3 Micro-mixing time definition

The correct definition of the micro-mixing time is a matter of importance for any EDC turbulent combustion model. The micro-mixing time definition taken in this study is applicable to the system with "natural" initial mixture non-uniformities and based on the β-model [2] proposed by Frisch [40, p.135-140]. In terms of this approach, at each stage of the Richardson cascade, the number of eddies formed from a given "parent" eddy is chosen such that the fraction of volume occupied by "active" eddies is decreased by a factor $\beta < 1$. In this way, the intermittency is introduced in a geometric form. The factor β is an adjustable parameter of the model. If l_o is the initial eddy size, and l is the size of the eddy formed on the n-th step of fragmentation, the fraction p_l of the active space can be calculated as

$$p_l = \beta^n = (\frac{l}{l_o})^{3-D}, \tag{7.29}$$

where the exponent D can be interpreted as a fractal dimension of the turbulent field. The expression (7.29) can be derived by considering the analytical representation of the Richardson cascade in the form:

$$f(x)f(y/x) = f(y)f(1), \tag{7.30}$$

where $f(1)$ is a number of eddies at the initial stage, $f(x) = f(l_o/\eta)$ is a number of η-fragments at the particular stage of fragmentation, $x = l_o/\eta$, $y = l_o/\xi$, η and ξ, $\xi < \eta$ are fragment sizes. he above equation has a general solution- the "fragmentation law"

$$N \equiv f(x) = Cx^D, \tag{7.31}$$

where C and D are the solution parameters, N is the number of fragments. The fraction of the "active" volume can be calculated as

$$\begin{aligned} Vol_N &= f(x)\eta^3 = C(l_o/\eta)^D\eta^3 \\ &= Cl_o^D\eta^{3-D} = Cl_o^3(\eta/l_o)^{3-D} \end{aligned}$$

[2] This β has nothing in common with that mentioned in the review paper [31].

This relation is identical to the expression (7.29). Since the active eddies of size $\sim l$ fill only a fraction p_l of a total volume, the specific energy associated with this scale is

$$E_l = {v_l}^2 p_l = {v_l}^2 (\frac{l}{l_o})^{3-D} \tag{7.32}$$

assuming the energy flux from scales $\sim l$ to smaller scales is $\sim E_l/\tau_l$, where $\tau_l = l/v_l$ is the eddy turnover time.

In the inertial range of scales, the energy flux is independent of l, i.e.,

$$\epsilon = v_o^3/l_o,$$

where ϵ is a dissipation rate of turbulent kinetic energy. After some algebra, one can get the expression for the eddy turnover time

$$\tau_l = \frac{l_o}{v_o}(\frac{l}{l_o})^{\frac{2}{3}+\frac{3-D}{3}} \tag{7.33}$$

The viscous cutoff scale of the β-model is obtained by equating the eddy turnover time and the viscous diffusion time $\tau_d = \eta_d^2/\nu$ that gives an expression for the dissipation scale

$$\eta_d = l_o Re^{-\frac{3}{1+D}}, \tag{7.34}$$

where $Re = l_o v_o/\nu$, and ν is molecular viscosity. When $D = 3$, the classic Kolmogorov expression is recovered; indeed, this assumption neglects the intermittency.

f l_o is defined in terms of $k-\epsilon$ model of turbulence, from Eq. (7.34), the viscous dissipation time can be derived as

$$\begin{aligned} \tau_d = \tau_{mix} &= (\frac{k}{\epsilon})^{\alpha}[(\frac{\nu}{\epsilon})^{1/2}]^{(1-\alpha)} \\ &= (\frac{k}{\epsilon}) \cdot (c_\mu/Re_t)^{\frac{1-\alpha}{2}}, \end{aligned} \tag{7.35}$$

where $\alpha = \frac{3(D-3)}{1+D}$, and k and ϵ are the turbulent kinetic energy and energy dissipation rate, respectively. From experiments reported in [41] follows that the fractal dimension for turbulent dissipation is about D=2.7, i.e

$$\tau_{mix} = (\frac{k}{\epsilon}) \cdot (c_\mu/Re_t)^{0.\overline{621}}$$

In particular, the eddy break-up time $\sim k/\epsilon$ corresponds to D=5, and Kolmogorov micro-scale time $\tau_k = (\nu/\epsilon)^{1/2}$ - to D=3.

Another approach developed is based on the usage of Kolmogorov expression for the micro-mixing time with the molecular viscosity replaced by a fraction of the effective viscosity assumed to be responsible for micro-mixing. If, for example, the RNG $k-\epsilon$ model is employed, the turbulent viscosity related to k, the turbulent kinetic energy, and ϵ, the dissipation rate of k, is given by the general expression.

$$\begin{aligned} \mu_t &= \mu_l(1+\sqrt{\frac{c_\mu \rho k^2/\epsilon}{\mu_l}})^2 \\ &= \rho(\nu_l + {\nu^s}_t + 2\sqrt{\nu_l {\nu^s}_t}), \end{aligned} \tag{7.36}$$

where ${\nu^s}_t$ is the "standard" k-ϵ value of the kinematic viscosity.

Provided that the first two terms in the expression (7.36) contribute to conventional diffusion transport, the geometrical mean [3] term can be assumed to determine the characteristic

[3]The micro-mixing time of such a form has been proposed (without deviation) in [26].

time scale for micro-mixing in the turbulence/chemistry interaction model, if written in a form similar to the Kolmogorov time definition, τ_k= $(\nu_l/\epsilon)^{1/2}$ replacing the molecular viscosity by a corresponding expression for the turbulent viscosity, i.e.,

$$\tau_{mix} = (2\sqrt{\nu_l \nu_t^s}/\epsilon)^{1/2} = (2\sqrt{c_\mu}\frac{k}{\epsilon}\tau_k)^{1/2}, \tag{7.37}$$

where c_μ=0.09 is the constant of the k-ϵ model of turbulence.

The above expression formally corresponds to D=3.8 in the general formula (7.35) giving only a provisional value for τ_{mix} that must be refined in comparisons with experiments. The model is assumed to be valid across a full range of flow conditions from low to high Reynolds numbers, if k and ϵ are determined from the generalized transport equations of the RNG k- ϵ model of turbulence implemented in the code [43].

Bibliography

[1] Sirignano, W.A., Fluid Dynamics and Transport of Droplet and Sprays, Cambridge University Press (2000)

[2] Kuo, K.K., ed., Recent Advances in Spray Combustion: Spray Combustion Measurements and Model Simulations, Vol.II, in Progress in Astronautics and Aeronautics, Vol. 171 (1996)

[3] Williams, F.A., Combustion Theory, 2nd ed., Addison-Wisley Publishing Co., Inc, London (1985)

[4] Kawano, D., Senda, J., Wada, Y., et al., Numerical Simulation of Multicomponent Fuel Spray, SAE Paper 2003-01-1838 (2003)

[5] Torres, D.J., Rourke, P.J., and Amsden, A.A., A Discrete Multicomponent Fuel Model for GDI Engine Simulations, ILASS Americas, 14th Annual Conference on Liquid Atomization and Spray Systems, Deaborn, MI (May 2001)

[6] Veynante, D., Vervisch, L., Turbulence Combustion Modeling, Progress in Energy and Combustion Science, 28: 193-266 (2002)

[7] Borghi, R., Turbulent Combustion Modeling, Progr. Energy Combust. Sciences., 14:245-292 (1988)

[8] Magnussen, B.F., Hjertager, B.H., On the Numerical Modeling of Turbulent Combustion with Special Emphasis on Soot Formation and Combustion, Sixteenth Symposium (International) on Combustion, Pittsburgh: The Combustion Institute, p. 719-729 (1976)

[9] Kralj,C., Numerical Simulation of Diesel Spray Processes, Ph.D. thesis, Imperial College, London (October 1995)

[10] Kong, S.F., Marriot, C.D.,Reitz, R.D., and Christensen, M., Modeling and Experiments of HCCI Engine Combustion Using Detailed Chemical Kinetics with Multidimentional CFD, SAE Paper 2001-01-1026 (2001) 4

[11] Fluent-6: Applications: Reacting flows,http:// www.fluent.com /software /fluent /application /reacting.htm (2002)

[12] Aubry, C., and Villermaux, J., J. Chemical Engineering Science, 30, p. 457 (1975)

[13] Golovitchev, V.I., Nordin,N., Jarnicki,R., and Chomiak, J., 3-D Diesel Spray Simulations Using a New Detailed Chemistry Turbulent Combustion Model, SAE Paper 2000-01-1891 (2000)

[14] Liang, P.Y., and Ungewitter, R.J., Multi-Phase Simulations of Coaxial Injector Combustion, AIAA Paper 92-0345 (1992)

[15] Appel,J., Bockhorn,H., and Frenklach,M., http: // www.me.berkeley.edu/soot/ mechanisms/abf.html (1999)

[16] Kee,R.J., Rupley,F.M., and Miller,J.A., Chemkin-II: A Fortran Chemical Kinetics Package for the Analysis of Gas Phase Kinetics, Sandia Report SAND89-8009B, UC-706 (April 1992)

[17] *Frisch, U.*, Turbulence, the Legacy of A.N. Kolmogorov, Cambridge University Press (1995)

[18] *Sreenivasan, K.R., and Meneveau, C.*, The fractal facet of turbulence, J. Fluid Mech.: vol. 173, pp. 357-386 (1986)

[19] Amsden A.A., KIVA-3: A KIVA Program with Block-Structured Mesh for Complex Geometries, LA-12503-MS (1993)

[20] Amsden A.A., KIVA-3v: A Block-structured KIVA Program for Engines with Vertical or Canted Valves, LA-13313-MS, July (1997)

[21] Curran,H.J., Gaffuri,P., Pitz,W.J., and Westbrook, C.K., A Comprehensive Modeling Study of n-Heptane Oxidation, Combustion and Flame, 114: 149 -177 (1998)

[22] Howard, J.B., http://web.mit.edu/anish/www/ MITcomb.html(2001)

[23] Golovitchev, V.I., http://www.tfd.chalmers.se / ~ valeri/MECH (1998)

[24] Wiartalla,A., Bäker,H., Brüggeman,D. and Koss, H., Influence of Spray Development and Fuel Quality on Soot Formation and Oxidation, JOULE-0008-D (AM) Report (1992)

[25] Golovitchev, V.I., Nordin, N., Detailed Chemistry Sub-Grid Scale Model of Turbulent Spray Combustion for the KIVA Code, Paper 99-ICE-237, ICE-Vol. 33-3: p.17-25 (1999)

[26] Karlsson, J., Modeling Auto-Ignition, Flame Propagation and Combustion in Non- Stationary Turbulent Sprays, Chalmers University of Technology, PhD Thesis, Göteborg (May 1995)

[27] Edwards, C.F., Siebers, D.L., and Hoskin, D.H., A Study of the Autoignition Process of a Diesel Spray via High Speed Visualization. SAE Paper 920108 (1992)

[28] Onishi, S., Jo, S.H., Shoda, K., Jo, P.D., and Kato, S., Active Thermo-Atmospheric Combustion (ATAC)-a New Combustion Process for Internal Combustion Engines, SAE Paper 790501 (1979)

[29] Frenklach, M., et al, http:// www.me.berkeley. edu/gri_mech (2000)

[30] Marinov, N. M., et al, http: www-cms.llnl.gov/ combustion/ nbutane_mech.txt (2000)

[31] *Golovitchev. V.I., and Chomiak, J.*, Evaluation of Ignition Improvers for Methane Autoignition, Comb. Sci. and Tech.: 135, 31 (1996)

[32] *Lifshitz, A., Scheller, K., and Burcat, A.*, Shock-Tube Investigation of Ignition in Methane-Oxygen-Argon Mixtures. Combustion and Flame, 16, 311 (1971)

[33] *Petersen, E.L., Davidson, D.F., Röhrig, M., and Hanson, R.K.*, Shock-Induced Ignition of High-Pressure H_2-O_2-Ar and CH_4-O_2-Ar Mixtures, 31st AIAA/ASMe/SAE/ASEE Joint Propulsion Conference and Exhibition, July 10-12, AIAA Paper 95-3113 (1995)